

**This accepted author manuscript is copyrighted and published by Elsevier. It is posted here by agreement between Elsevier and MTA. The definitive version of the text was subsequently published in Polymer, 55, 26, 2014, DOI: 10.1016/j.polymer.2014.10.056. Available under license CC-BY-NC-ND.**

**Dielectric relaxations in polyoxymethylene and in related nanocomposites: identification and molecular dynamics**

P. K. Karahaliou<sup>1,\*</sup>, A. P. Kerasidou<sup>1</sup>, S. N. Georga<sup>1</sup>, G. C. Psarras<sup>2</sup>, C. A. Krontiras<sup>1</sup> and J. Karger-Kocsis<sup>3-4</sup>

<sup>1</sup> Department of Physics, University of Patras, Patras 26504, Greece

<sup>2</sup> Department of Materials Science, University of Patras, Patras 26504, Greece

<sup>3</sup> Department of Polymer Engineering, Budapest University of Technology and Economics, H-1111 Budapest, Múgyetem rkp. 3, Hungary

<sup>4</sup> MTA-BME Research Group for Composite Science and Technology, Múgyetem rkp. 3., Budapest H-1111, Hungary

\*Corresponding author: [pkara@upatras.gr](mailto:pkara@upatras.gr)

## **Abstract**

Broadband dielectric spectroscopy is employed for the study of the dielectric response of **Polyoxymethylene**/boehmite alumina (POM/alumina) and Polyoxymethylene/Layered Silicates (POM/LS) semi-crystalline nanocomposites, together with the response of pure POM. The compilation of the dielectric responses **of all systems** reveals the existence of five dielectric relaxation mechanisms assigned, in terms of decreasing temperature at constant frequency, as IP (interfacial polarization),  $\alpha$ -

$\beta$ -,  $\gamma$ - and  $\delta$ -relaxations. IP,  $\alpha$ - and  $\gamma$ -relaxations are detected in all studied systems and they are well documented in the literature.  $\delta$ -relaxation, been the fastest mechanism, is present only in the POM/LS system and is associated with defect dipoles in the crystalline phase of POM. Finally,  $\beta$ -relaxation is present only in the POM/alumina nanocomposite and its dynamics obey Vogel–Fulcher–Tamann temperature dependence. This work presents a complete mapping of the dielectric relaxation mechanisms of POM and signifies the connection of  $\beta$ -mode with the glass to rubber transition of POM, confirming its cooperative character.

Keywords: polyoxymethylene, dielectric relaxation, nanocomposites, layered silicates, boehmite alumina

## 1. Introduction

Polyoxymethylene (POM) is a well known semicrystalline polymer which belongs to the so called engineering thermoplastics, due to its huge number of applications ranging from high performance engineering components to tiny precision parts in drug delivery systems. Its suitability in numerous applications is mainly due to its low friction and wear characteristics, its excellent thermomechanical performance and its resistance to various solvents and fuels, together with its low cost [1]. POM also exhibits good electrical insulation characteristics and low water absorption that makes it useful in electrical and electronic applications that require long-term stability [1]. Nevertheless, POM also possesses high degrees of crystallinity that translates into undesirable properties, such as brittleness and high melt shrinkage, which limit its applications. To overcome this problem the scientific interest is

focused to the preparation and study of POM blends and POM based composite materials attaining superior properties with possible utilization for electrical applications [1-2].

The relaxation mechanisms of POM and POM based systems have been the subject of extended studies, via various techniques, since 1960s and their interpretation constitutes a challenging issue in the literature [1-18]. So far, at least three distinct relaxations have been identified, dielectrically and/or mechanically, in POM containing systems. These are assigned in the literature, in terms of decreasing temperature at constant frequency, as  $\alpha$ ,  $\beta$  and  $\gamma$  relaxations and their molecular origins have been extensively discussed and debated. The origin of  $\alpha$ - and  $\gamma$ -mode is quite well explored and understood:  $\alpha$ -relaxation takes place in the crystalline regions of POM [3-6, 9, 11, 13-15], while  $\gamma$ -relaxation is associated with the amorphous phase [3-5, 8, 14-15]. On the other hand, the physical origin of  $\beta$ -relaxation appears controversial in the early literature [3, 7, 8, 10, 12, 14-15]. The majority of researchers agree that this relaxation is related to the glass to rubber transition in the amorphous phase of POM [3-5, 10, 12, 14, 15, 16-18]. Nevertheless, there are arguments against this assignment [6, 19]. The latter are supported by the fact that  $\beta$ -relaxation appears very weak or it is even not detected experimentally in any POM based system, especially by means of dielectric relaxation [3, 14-15]. This impeded the clarification of the physical origin of  $\beta$ -mode as well as its cooperative character, through its electrical relaxation dynamics.

Within the framework of the present study POM/Boehmite Alumina (POM/alumina) and POM/Layered Silicate (POM/LS) nanocomposites are studied by means of broadband dielectric spectroscopy. POM matrix is also studied as a reference system. Our working hypothesis is that the insertion of the nano-inclusions in the polymer matrix drastically affects the dielectric response of the pure POM by revealing the evolution of dielectric mechanisms not detectable in the pure system but

still originating from it. Additionally, the compilation of the dielectric responses of all three studied systems offers the opportunity to draw a complete dielectric relaxation map for POM over a wide temperature and frequency range. Finally, a major outcome of the current study appears to be the elucidation of the cooperative character of  $\beta$ -relaxation and its unambiguous association with the glass to rubber transition of the amorphous phase of POM. This is achieved by analyzing its dynamics, through the dielectric data, over a wide frequency and temperature range.

## **2. Materials and methods**

Granulated POM (Hostaform C 9021, Ticona GmbH, Frankfurt, Germany) was used as polymeric matrix for all composite systems. Its volumetric melt flow rate (MVR at 190°C/2.16 kg) was 8 cm<sup>3</sup>/10 min. Water-dispersible boehmite alumina (AlO(OH), Disperal® 11N7-80, supplied by Sasol, Hamburg, Germany) with specific surface area of 100 m<sup>2</sup>/g and mean particle diameter of 220 nm and synthetic sodium fluorohectorite (Somasif ME-100) of Co-op Chemicals (Tokyo, Japan) used as LS, with intergallery distance of 0.95 nm and very high aspect ratio of viz. >1000, served as fillers for the preparation of the nanocomposites. POM/alumina and POM/LS binary systems were prepared by water mediated-continuous technique (WM-CT) in a twin-screw extruder. The alumina and layered silicates contents, in the binary composites, were set at 3 wt%. The details of the preparation procedure can be found elsewhere [20-22].

The electrical characterization of all three systems was performed by means of Broadband Dielectric Spectroscopy (BDS) in the frequency range from 10<sup>-1</sup> Hz to 1MHz using the Alpha-N Frequency Response Analyser and the BDS-1200 parallel-plate capacitor test cell, with two gold-plated electrodes, supplied by Novocontrol Technologies (Hundsagen, Germany). Measurements were

performed in the temperature range from  $-100$  to  $150$  °C in steps of  $10$ °C. The temperature was controlled by the Quattro system (Novocontrol Technologies Hundsagen, Germany) within  $\pm 0.1$  °C. The dielectric cell was electrically shielded within a nitrogen gas atmosphere and isothermal frequency scans were conducted for each of the specimens examined with the application of an AC voltage of  $V_{rms}=1.0$  V. The system was fully automated and the WinDeta software was used for system control and data acquisition.

### 3. Results and Discussion

The dielectric response of POM, POM/alumina and POM/LS systems is presented in Figs. 1a-1c respectively, in terms of the loss tangent,  $\tan\delta$ , as a function of frequency ( $f$ ) and temperature ( $T$ ). Relaxation mechanisms are detected quite pronouncedly by the formation of relaxation peaks in the  $\tan\delta$  ( $f$ ,  $T$ ) representation. A common feature of all 3D plots of figure 1 is the high values of the loss tangent, together with a tendency for a loss peak formation. In the same frequency and temperature region a steep increase of the real part of the permittivity (not shown here), is recorded. This is characteristic of the presence of interfacial phenomena such as interfacial and/or electrode polarization, due to accumulation of charges, as well as increased conductivity [5, 23-25]. This low frequency-high temperature response should be attributed, in the systems under study, to interfacial polarization phenomena rather than increased conductivity. This hypothesis is supported by the fact that accumulation of free charges can take place not only at the interfaces of POM with alumina or layered silicates but also at the interfaces of the crystalline with the amorphous regions of POM. In favor of that are the results of previous reports in POM containing systems, where high degrees of crystallinity, reaching up to 83%-85%, have been evaluated [7, 9]. Additionally, the measured

conductivity values, in this frequency and temperature range, remain low ( $\sim 1 \times 10^{-9}$  S cm<sup>-1</sup> at 150 °C and 0.1 Hz) for all studied systems.

In the temperature range from 50°C to 150 °C another slow relaxation mechanism is detected, in all studied systems, which is denoted as  $\alpha$ -mode of POM (Figs. 1a, 1b and 1c) in accordance with our previously reported results on POM containing systems [21, 23, 26]. A third common feature of all examined systems is the clear formation of a fast relaxation mechanism, in the temperature range between -100 °C and -40 °C (Figs. 1a, 1b and 1c). This mechanism is denoted as  $\gamma$ -mode of POM and is also present in all POM containing systems previously studied by the authors [21, 23, 26]. Both  $\alpha$ - and  $\gamma$ -modes of POM have been previously detected dielectrically as well as mechanically too [3-5].

The high temperature  $\alpha$ -mode is mostly marked in the mechanical results, while its manifestation in the dielectric spectroscopy results is suppressed by the elevated values of both real and imaginary parts of the dielectric permittivity. It is well established that this relaxation mechanism is associated with the crystalline phase and attributed to translational motions along the polymer chain which take place at the surface of the crystallites [3, 5]. The origin of  $\gamma$ -relaxation of POM has been a highly debated topic. Some researchers have attributed this mechanism to the glass to rubber transition of POM [6], an argument which was also supported by calorimetric studies [19]. However, subsequent studies suggested that  $\gamma$ -relaxation is associated with local motions not affected by changes introduced by crystallization [15-16]. Accordingly, the debate about  $\gamma$ -mode seemed to be resolved and this relaxation is generally accepted as a mechanism connected with the hydroxyl end groups and/or local twisting motions of the mainchain that mainly take place in the disordered regions of the bulk polymer [3-4, 15-16]. However, the existence of a relaxation related to the glass to rubber

transition, as well as the concept of the glass transition in high crystallinity polymers, remains an open issue [1, 3, 5, 15].

While only three relaxation mechanisms are detected in the pure POM system, namely IP,  $\alpha$ -relaxation and  $\gamma$ -relaxation, additional relaxations appear in the dielectric spectra of POM/alumina and POM/LS systems. In the case of POM/alumina nanocomposites, an additional relaxation peak is observed at intermediate frequencies and in the temperature range between  $-40\text{ }^{\circ}\text{C}$  and  $30\text{ }^{\circ}\text{C}$  (Fig. 1b). This relaxation is denoted as  $\beta$ -mode, since it is faster than  $\alpha$ -relaxation but slower than  $\gamma$ -mechanism. The physical origin of this mechanism cannot be ascribed unambiguously. On one hand this relaxation process is only present in the POM/alumina system while it is not detected in any other POM containing system included not only in this work but also in previously reported works [21-23, 26]. For that reason this process can be initially attributed to the alumina filler itself. Such intermediate mechanisms have been observed in polymer matrix/ ceramic filler composites and are attributed to polarization phenomena that take place within the reinforcing phase [24-25, 27]. On the other hand, previous studies by us on alumina containing composites embedded in a PU polymer matrix (PU/alumina composites) [28], do not reveal the existence of such mechanism that can be attributed to polarization within the alumina filler. In order to clarify the origin of  $\beta$ -relaxation recorded in the POM/alumina composite one should recall the results of Dynamic Mechanical Analysis (DMA) reported for the pure POM, POM blends [3, 22, 15, 29] as well as for the POM/alumina composites of this study [22]. In all cases included in the aforementioned studies, the DMA results suggest the existence of a relaxation mechanism in the same temperature range with the one that  $\beta$ -mode is observed in the POM/alumina system of this work. Furthermore, in some of the above studies it is suggested that  $\beta$ -mode is affected by changes in crystallinity, a fact that implies a cooperative character of the

corresponding mechanism [3, 15, 30]. While, the mechanical  $\beta$ -peak of POM has been repeatedly reported in the literature, the dielectric  $\beta$ -mode appears very weak or is completely absent in studies of pure POM [3, 15, 31-32]. Its presence is strengthened in POM containing copolymers and blends [10, 15, 33-35], due to the reduction of crystallinity of these systems relative to pure POM [15]. As a result  $\beta$ -relaxation appears as a mechanism affected by changes in crystallinity that is of cooperative character, contrary to  $\gamma$ -relaxation which is not affected due to its localized nature [15]. These arguments lead to the assumption that  $\beta$ -relaxation is a process that could be associated to the glass to rubber transition of POM. The latter remains yet to be confirmed, since it is well known that a dielectric process associated to the glass to rubber transition follows, as a cooperative mode, a Vogel–Fulcher–Tamann (VFT) type temperature dependence [5]. Adams and Gibbs [36], were the first to introduce the idea of cooperative character for the relaxation mechanism associated to the glass to rubber transition and connect it with a non-Arrhenius behavior, such as the VFT equation. Under their assumption the cooperativity results from segmental regions of the polymer (cooperative regions), rearranging thus from one configuration into another independently of their environment, upon an energy fluctuation [36].

The loss spectrum of Fig. 1c, which corresponds to the POM/LS composite system, appears even more complex. Apart from the IP,  $\alpha$ - and  $\gamma$ -relaxation of POM, an even faster relaxation mechanism is recorded in the low temperature region between -100 °C and -70 °C. This is denoted as  $\delta$ -mode and it is also attributed to the POM matrix. It should be mentioned here that the same low-temperature and high frequency mechanism, assigned here as  $\delta$ -mode, has also been detected in ternary composite systems of POM and PU reinforced with layered silicates [37], while it is absent from



the dielectric spectra of rubber/layered silicates nanocomposites previously reported by the authors [38].

In order to assign this  $\delta$ -relaxation, one should recall the rapid broadening of  $\gamma$ -peak, present in numerous cases for POM and polyethylene (PE) containing systems, with decreasing temperature [3-5]. It has been suggested that this broadening can be interpreted in terms of two coexisting relaxation mechanisms, i.e local relaxation motions in noncrystalline phase in tandem with relaxations due to defects or dislocations in the crystallites [4-5, 10]. There are also cases of dielectric and mechanical relaxation processes of POM or PE containing systems where  $\gamma$ -peak is readily resolved into two maxima [8, 10, 39]. The first maximum is located around -70 °C and corresponds to the main contribution of  $\gamma$ -mode to the dielectric or mechanical spectra, as it involves motions of short segments in the disordered regions of POM. A mechanism associated with defects in the crystalline phase of POM is proposed by Hojfors et al. [10] for the second maximum located at lower temperatures (around -100 °C) where breaking away of dislocations from their pinning points under mechanical stresses occurs.

In the case of the present study, the inclusion of LS within the POM polymer matrix seems to emerge the evolution of the electrically active  $\delta$ -mode, which is hindered in the cases of pure POM and POM/alumina systems. The inclusion of LS results in the following morphological configurations: (i) composites where matrix and LS remain immiscible (microphase separated composites) (ii) composites where polymer molecules are inserted between the silicate layers (intercalated structures) and (iii) structures where individual silicate layers are dispersed in the polymer matrix (exfoliated structures) [38]. The intercalation or exfoliation of silicate layers introduce line defects into the crystalline phase of POM, which act as areas where the local electric field is distorted allowing the appearance of electrical

dipolar moments able to reorient following the variation of the applied electric field, thus resulting in the presence of  $\delta$  -mode. These electrical dipole moments are referred as defect dipoles and can be extremely large [40].

Finally, in the loss spectrum of Fig. 1c and in intermediate temperatures and frequencies the trace of another relaxation mechanism is detected denoted as IDE (Intermediate Dipolar Effect). Similar relaxation mechanisms have been previously reported for polymer matrix / inorganic filler composites and have been attributed to polarization phenomena taking place within the reinforcing phase [24-25, 27]. Since this relaxation is attributed to the layered silicate itself, its analysis is beyond the scopes of the current work.

In Fig. 2, isothermal plots of the imaginary part of the electric modulus,  $M''$ , versus frequency are presented for all three examined systems and for three different temperatures in the low temperature region, for reasons of comparison. The loss peaks of  $\delta$ -,  $\gamma$ - and  $\beta$ -relaxations of POM are recorded successively, in order of decreasing frequency or increasing temperature. It is obvious (Fig. 2a) that the broad peak corresponding to  $\gamma$ -relaxation is not affected by the inclusion of alumina filler to the POM matrix, as far as the shape and the position of the loss maximum is concerned. On the contrary, the incorporation of LS into the POM results in a slight shift of the loss maximum of  $\gamma$ -relaxation to higher frequencies together with the appearance of the faster  $\delta$ -relaxation in the high frequency regime of the POM/LS spectrum. At the temperature of -50 °C (Fig. 2b) the shift of the loss maximum of the  $\gamma$ -relaxation is also present, while the faster  $\delta$ -relaxation is shifted outside the measuring frequency window. The observed shift of the peak relaxation frequency of  $\gamma$ -mode, in the case of the POM/LS system, can be reasonably attributed to the coexistence of this mode with the faster  $\delta$ -relaxation or even to the merge of both relaxations at higher temperatures. Moreover, on the

low frequency edge of the POM/alumina spectrum the appearance of  $\beta$ -relaxation is evident, becoming more pronounced via the formation of a loss peak located at around 7Hz at  $-20\text{ }^{\circ}\text{C}$  (Fig. 2c).

Analogous comparative plots of all three studied systems are presented in Fig. 3a-3c, where the imaginary part of electric modulus,  $M''$ , is plotted in double logarithmic scale, for three different temperatures, i.e  $100\text{ }^{\circ}\text{C}$ ,  $120\text{ }^{\circ}\text{C}$  and  $150\text{ }^{\circ}\text{C}$ , respectively. The dielectric response of all POM containing systems is dominated by the formation of the relaxation peak corresponding to  $\alpha$ -mode. The inclusion of inorganic filler into the POM matrix results in the displacement of the loss peak maxima to lower frequencies, at constant temperature, by one and two orders of magnitude for the POM/alumina and POM/LS system, respectively. This shifting of  $\alpha$ -relaxation, observed in the present work dielectrically, is in accordance with an analogous shifting of  $\alpha$ -relaxation traced in the dynamic mechanical analysis of POM/alumina system [22]. In Figs. 3b and 3c, IP relaxation, appears as a shoulder in the low frequency edge of the spectra. IP relaxation is more pronounced in the case of pure POM than in the composites, in support of the argument that the electrical heterogeneity of the systems under study is introduced not only by the incorporation of the different fillers into the POM matrix, but mainly by the high degree of crystallinity of POM. Therefore, IP is related to different types of interfaces, i.e. interfaces between the matrix and the filler and interfaces between the amorphous and crystalline regions of POM.

The variation of the imaginary part of electric modulus,  $M''$ , as a function of temperature is presented in Figs. 4a and 4b, for frequencies of 0.1 Hz and 1kHz respectively, and for all three studied systems. In the isochronal plots of 0.1 Hz (Fig. 4a),  $\alpha$ -relaxation dominates the high temperature edge, while in the frequency of 1kHz (Fig. 4b),  $\alpha$ -peak of POM/alumina and POM/LS lay outside the measuring temperature window. As commented before,  $\alpha$ -relaxation of POM shifts to lower frequencies isothermally (Fig. 3) or to higher temperatures isochronically (Fig. 4) with the inclusion of

alumina or LS fillers. Shift of the  $\alpha$ -peak to higher temperatures, has been previously observed for POM following annealing, attributed to the increase of the crystallite size [6, 22]. Nevertheless, previous morphological and thermal studies on POM/alumina systems, similar to the one studied in the present work, do not indicate any change in the crystalline structure of POM due to the incorporation of the alumina slurry [20]. As a result we cannot attribute the shift of  $\alpha$ - peak to crystallinity changes. Isochronal shift to higher temperatures of the  $\alpha$ -relaxation of low density polyethylene (LDPE)-chalk composites, as a function of filler concentration, has been reported elsewhere [41]. In that work, it is mentioned that the crystallinity of the samples is not affected by the inclusion of the filler or the increase of the filler concentration. It is rather suggested that the presence of the filler disturbs the amorphous-crystal interface in such a way that the nanofiller acts like a stretching agent for the chains located at the interface. Regarding that the crystallinity of the specimens, examined in the present work, is not affected by the inclusion of the filler [20], a similar interpretation can be adopted for the  $\alpha$ -peak shift observed in our measurements.

It is also evident that  $\beta$ -relaxation is present only in the POM/alumina system (Figs. 4a and 4b), while  $\delta$ -mode is present only in the POM/LS system (Fig. 4b) and only in a limited temperature and frequency window.

The dynamics of all relaxation mechanisms detected in POM and POM containing systems of the current study are presented in Fig. 5. Loss peak frequencies of the IP relaxation are not included in the graph, since IP relaxation is superimposed with  $\alpha$ - relaxation and the corresponding peaks cannot be deconvoluted, undoubtedly. All three  $\alpha$ -,  $\gamma$ - and  $\delta$ -relaxations follow an Arrhenius-type temperature dependence given by:

$$f_{\max} = f_0 \exp\left(-\frac{E_A}{k_B T}\right), \quad (1)$$

with  $E_A$  being the activation energy,  $f_0$  a pre-exponential factor and  $k_B$  the Boltzmann constant. The activation energies of all three  $\alpha$ -,  $\gamma$ - and  $\delta$ - relaxations are evaluated by fitting the experimental data to equation (1) and are listed in Table I.

On the other hand  $\beta$ -relaxation deviates from the Arrhenius behavior and obeys a VFT temperature dependence, following the expression:

$$f_{\max} = f_0 \exp\left(-\frac{AT_0}{T-T_0}\right), \quad (2)$$

where  $f_0$  is a pre-exponential factor,  $A$  is a constant (being a measure of the activation energy) and  $T_0$  the Vogel temperature or ideal glass transition temperature. The VFT parameters are evaluated by fitting equation (2) to the experimental results obtained for  $\beta$ -relaxation in the POM/alumina system and are listed in Table I. The VFT temperature dependence of the loss maxima in the case of  $\beta$ -relaxation indicates a cooperative character of the corresponding relaxation mechanisms, which is typical behavior for mechanisms related to the glass to rubber transition of the amorphous phase [5, 42]. This result confirms the initial hypothesis of ours that  $\beta$ -relaxation, recorded only in the POM/alumina system, is related to the glass to rubber transition of POM. The reason why this relaxation is present neither in pure POM nor in the POM/LS system is not clear. However, a possible explanation might be drawn taking into account the differences between the chemical character of alumina and LS along with their interactions with POM. A typical picture of the chemical structure of layered silicates includes few surface  $-OH$  groups located at the edges of the layers [43]. On the other hand boehmite alumina exhibits a large number of surface  $-OH$  groups located everywhere [44, 45]. In both cases interactions via weak H-bonding are possible between the  $-OH$  groups and  $-O$  atoms of

POM in the amorphous phase. Since, more –H bonds are present between POM and boemite alumina, compared to those between POM and LS, the molecular segments within the amorphous phase of POM are more flexible in the case of POM/alumina system. In the cases of pure POM or POM/LS the amorphous segments are more confined and rigid. This might be the reason why  $\beta$ -relaxation appears in the case of POM/alumina system and not in the case of pure POM or POM/LS systems.

The calculated activation energies (Table I) lay between 0.96-1.15 eV (22-26.5 kcal mol<sup>-1</sup>) for  $\alpha$ -relaxation and between 0.64-0.86 eV (14.8-19.8 kcal mol<sup>-1</sup>) for  $\gamma$ -relaxation. These values are in good agreement with previously reported values of activation energies for the dielectric  $\alpha$ - and  $\gamma$ - processes, which lay between 20-24 kcal mol<sup>-1</sup> and 19.3-20 kcal mol<sup>-1</sup>, respectively [3].

Interestingly, comparing the value of the activation energy of  $\alpha$ -process in pure POM with those calculated for the same process in the cases of the nanocomposites, a decrease of the activation energy is observed. This implies that the presence of the filler facilitates the corresponding mechanism. The opposite trend is observed in the case of  $\gamma$ -relaxation, where a higher activation energy was found for the POM/LS system (0.86 eV) than for the pure POM and POM/alumina. The activation energy of the latter systems ranges between 0.64-0.68 eV. The higher activation energy of POM/LS might be connected with the presence of the extra high frequency  $\delta$ -relaxation detected only in this system, in a sense that  $\gamma$ -relaxation is obstructed by the presence of another process ( $\delta$ -relaxation) appearing at higher frequencies.

**Table 1.** Activation energies for  $\alpha$ -,  $\gamma$ - and  $\delta$ -relaxations of POM, evaluated through eq. (1) and fitting parameters of eq. (2) for  $\beta$ -relaxation of POM, detected in all three POM containing systems.

Sample	$\alpha$ -mode	$\beta$ -mode	$\gamma$ -mode	$\delta$ -mode
--------	----------------	---------------	----------------	----------------

	$E_A$ (eV) [kcal mol <sup>-1</sup> ]		$E_A$ (eV) [kcal mol <sup>-1</sup> ]	$E_A$ (eV) [kcal mol <sup>-1</sup> ]
<b>POM</b>	1.16 [26.75]		0.68 [15.68]	-
<b>POM/alumina</b>	1.04 [23.98]	$T_0=190$ K, $A=3$	0.64 [14.76]	-
<b>POM/LS</b>	0.96 [22.14]	-	0.86 [19.83]	0.54 [12.45]

### Summary and conclusions

This work presents a comparative study on the dielectric response of pure POM with POM/alumina and POM/LS nanocomposites. This material selection offers the opportunity to draw, for the first time to the best of our knowledge, a full record and identification of the dielectric relaxation mechanisms present in POM. This is illustrated in Fig. 6a, where the imaginary part of electric modulus,  $M''$ , is plotted versus frequency and temperature, for all three studied systems in a common 3D plot, as well as via the combined Cole-Cole plots of Fig. 6b, where all occurring relaxation mechanisms are shown successively from the slowest to the fastest one.

Specifically, three relaxation mechanisms are recorded in the case of pure POM. These are, in terms of increasing temperature, the well established  $\gamma$ - and  $\alpha$ -relaxations of POM and the IP mode in the low frequency edge of the spectra. Among them,  $\alpha$ -relaxation is connected to the crystalline phase and involves translational motions along the chain axis,  $\gamma$ - relaxation is associated with the amorphous phase and corresponds to localized motions at the disordered regions of the bulk, while IP mode is connected to interfacial phenomena taking place mainly at the interfaces of the amorphous with the crystalline regions.

The incorporation of nano-inclusions within the polymeric POM matrix results in the mobilization of two extra relaxation mechanisms also attributed to POM. In the case of the POM/alumina nanocomposite an extra relaxation mechanism is recorded at intermediate temperatures (-30 °C to 40 °C), which is denoted as  $\beta$ -mode of POM and obeys a VFT temperature dependence. The latter implies a cooperative character of the corresponding mechanism and as a result an association of  $\beta$ -mode to the glass to rubber transition is concluded. To the best of our knowledge this is the first time that  $\beta$ -mode of POM is recorded dielectrically in such wide temperature and frequency range, allowing us to determine the VFT parameters. Thus, the connection of  $\beta$ -mode to the glass to rubber transition of POM becomes unambiguous.

Moreover, the inclusion of layered silicates into the POM matrix emerges a low temperature fast relaxation mechanism that is not present in the pure POM or the POM/alumina nanocomposites and it is attributed to the reorientation of dipolar moments connected to the presence of defects in the crystalline phase of POM (defect dipole moments). Analogous relaxation mechanisms have been scarcely observed dielectrically and are mostly marked in the DMA results typically in coexistence with  $\gamma$ -relaxation either in one broad relaxation peak or with the formation of a second peak, whose deconvolution from  $\gamma$ -relaxation is difficult. The important finding of the current work is that in the case of POM/LS system,  $\delta$ -relaxation appears in the dielectric loss spectra through the formation of a clear relaxation peak, well separated from  $\gamma$ -peak and in such a way that its dynamics can be explicitly analyzed and its activation energy can be easily determined.

To summarize, the combined analysis of the dielectric response of three POM containing systems, namely POM, POM/alumina and POM/LS resulted in: (i) the clarification of the nature of  $\beta$ -relaxation observed in POM, verifying that this mechanism is connected to the glass to rubber



transition, (ii) revealing the existence of a faster  $\delta$ -relaxation mechanism in the low temperature region, which was scarcely observed in previously studied POM containing systems and certainly without the clarity that it is imprinted in our data (iii) offering a complete mapping of the dielectric relaxation response of POM.

## References

- [1] Lüftl S, Visakh PM and Chandran S, editors. Polyoxymethylene Handbook: Structure, Properties, Applications and their Nanocomposites (Polymer Science and Plastics Engineering) Massachusetts: John Wiley & Sons, Inc. Hoboken, New Jersey-Scrivener Publishing LLC; 2014.
- [2] Tjong SC and Mai Y-W, editors. Physical properties and applications of polymer nanocomposites. Philadelphia: Woodhead Publishing Limited; 2010.
- [3] McCrum N G, Read BE and Williams G. In: Anelastic and Dielectric Effects in Polymeric Solids, London: John Wiley and Sons; 1967. p.540-551.
- [4] Vassilikou-Dova A and Kalogeras IM. Dielectric Analysis (DEA). In: Menczel JD and Bruce Prime R, editors. Thermal analysis of polymers, fundamentals and applications. New Jersey: John Wiley & Sons, Inc. Hoboken; 2009.p. 497-613.
- [5] Kremer F and Schönhals A, editors. Broadband Dielectric Spectroscopy, Berlin: Springer; 2003.
- [6] Read BE. and Williams G. The Dielectric and Dynamic Mechanical Properties of Polyoxymethylene (Delrin). Polymer 1961; 2:239-255.
- [7] Porter CH, Lawler JHL, Boyd RH. A dielectric study of molecular relaxation in polyoxymethylene at high temperatures. Macromolecules 1970; 3(3): 308-314; Porter CH, Boyd RH. A Dielectric Study of the Effects of Melting on Molecular Relaxation in Poly(ethylene oxide) and Polyoxymethylene. Macromolecules 1971;4(5): 589-594.
- [8] Papir YS and Baer E. The Internal Friction of Polyoxymethylene from 4.2° to 300°K. Mater Sci Eng 1971;8(6):310-322.
- [9] Gray RW. On the  $\alpha$ -relaxation in bulk polyoxymethylene. J Mater Sci 1973; 8: 1673-1689.

- [10] Hojfors RJV, Baer E and Geil PH. Dynamic-mechanical study of molecular motions in solid polyoxymethylene copolymers from 4 to 315°K. *J Macromol Sci Phys B* 1977;13(3): 323-348.
- [11] Enns JB, Simha R. Transitions in semicrystalline Polymers. II. Polyoxymethylene and poly (ethylene oxide). *J Macromol Sci Phys B* 1977;13(1): 25-47.
- [12] Kazen ME, Geil PH. Electron Microscopy Studies of relaxation behavior of polyoxymethylene. *J Macromol Sci Phys B* 1977;13(3): 381-404.
- [13] Starkweather Jr HW. Simple and complex relaxations. *Macromolecules* 1981;14(5):1277-1281.
- [14] Boyd RH. Relaxation processes in crystalline polymers: experimental behavior-a review. *Polymer* 1985; 26 (3): 323-347; Relaxation processes in crystalline polymers: molecular interpretation - a review. *Polymer* 1985;26 (8):1123-1133.
- [15] Sauer BB, Avakian P, Flexman EA, Keating M, Hsiao BS and Verma RK. A.C. Dielectric and TCS studies of constrained amorphous motions in flexible polymers including poly(oxymethylene) and miscible blends. *J Polym Sci B: Polym Phys* 1997; 35(13):2121–2132.
- [16] Wasylshyn DA. Effect of moisture on the dielectric properties of polyoxymethylene (POM). *IEEE Trans Dielectr Electr Insul* 2005; 12:183–193.
- [17] Bershtein VA, Egorova LM, Egorov VM, Peschanskaya NN, Yakushev PN, Keating MY, Flexman EA, Kassal RJ, Schodt KP. Segmental dynamics in poly(oxymethylene) as studied via combined differential scanning calorimetry/creep rate spectroscopy approach. *Thermochimica Acta* 2002; 391:227–243.
- [18] Kumaraswamy G, Surve NS, Mathew R, Rana A, Jha SK, Bulakh NN, Nisal AA, Ajithkumar TG, Rajamohanan PR, Ram Ratnagiri. Lamellar Melting, Not Crystal Motion, Results in Softening of Polyoxymethylene on Heating. *Macromolecules* 2012; 45:5967-5978.

- [19] Suzuki H, Grebowicz J and Wunderlich B. Heat Capacity of Semicrystalline linear and poly(oxymethylene) and poly(oxyethylene). *Makromol Chem* 1985; 186 (5):1109-1119.
- [20] Siengchin S, Karger-Kocsis J, Thomann R. Nanofilled and/or toughened POM composites produced by water-mediated melt compounding: Structure and mechanical properties. *eXPRESS Polym Lett* 2008; 2(10): 746–756; Siengchin S and Karger-Kocsis J. Binary and ternary composites of polystyrene, styrene–butadiene rubber and boehmite produced by water-mediated melt compounding: Morphology and mechanical properties. *Composites B* 2013;45 : 1458-1463.
- [21] Siengchin S, Karger-Kocsis J, Psarras GC and Thomann R. Polyoxymethylene/polyurethane/alumina ternary composites: Structure, mechanical, thermal and dielectric properties. *J Appl Polym Sci* 2008; 110:1613–1623.
- [22] Siengchin S. Dynamic mechanic and creep behaviors of polyoxymethylene/boehmite alumina nanocomposites produced by water-mediated compounding: Effect of particle size. *Journal of Thermoplastic Composite Materials* 2013; 26: 863-877.
- [23] Psarras GC, Siengchin S, Karahaliou PK, Georga SN, Krontiras CA and Karger-Kocsis J. Dielectric relaxation phenomena and dynamics in polyoxymethylene/polyurethane/alumina hybrid nanocomposites. *Polym Int* 2011; 60:1715-1721.
- [24] Kontos GA, Soulintzis AL, Karahaliou PK, Psarras GC, Georga SN, Krontiras CA, Pisanias M N. Electrical relaxation dynamics in TiO<sub>2</sub> – polymer matrix composites. *Express Polym Lett* 2007; 1(12):781–789.
- [25] Soulintzis A, Kontos G, Karahaliou PK, Psarras GC, Georga SN, Krontiras CA. Dielectric Relaxation Processes in Epoxy Resin – ZnO Composites. *J Polym Sci Part B: Polym Phys* 2009; 47:445–454.

- [26] Siengchin S. Nano-Scale Reinforcing and Toughening Thermoplastics: Processing, Structure and Mechanical Properties. In: Tong L, editor., Nanofibers – Production, Properties and Functional Applications. InTech; 2011. p. 215-240.
- [27] Hernández M, Ezquerro TA, Verdejo R, and López-Manchado MA. Role of Vulcanizing Additives on the Segmental Dynamics of Natural Rubber. *Macromolecules* 2012; 45 (2):1070–1075.
- [28] Kalini A, Gatos KG, Karahaliou PK, Georga SN, Krontiras CA, Psarras GC. Probing the Dielectric Response of Polyurethane/Alumina Nanocomposites. *J Polym Sci Part B: Polym Phys* 2010; 48:2346–2354.
- [29] Siengchin S and Karger-Kocsis J. Mechanical and stress relaxation behavior of Santoprene® thermoplastic elastomer/boehmite alumina nanocomposites produced by water-mediated and direct melt compounding. *Compos A* 2010; 41: 768–773.
- [30] McCrum NG. Internal Friction in Polyoxymethylene. *J Polym Sci* 1961 ; 54 : 561- 568.
- [31] Ishida Y, Matsuo M, Ito H, Yoshino M, Irie F and Takayanagi M. Dielectric behavior and visco-elastic behavior of polyoxymethylene (Delrin) *Kolloid Z* 1961; 174: 162- 163.
- [32] Arisawa K, Tsuge K and Wada Y. Dielectric Relaxations in Polyoxymethylene and Polyethylene Oxide. *Jpn J Appl Phys* 1965; 4: 138-147.
- [33] Bohn L. Die Einfriertemperatur des Polyoxymethylens. *Kolloid-Z/Z Polymere* 1965;201:20-23.
- [34] French RN, Machado JM and Lin-Vien D. Miscible polyacetal-poly (vinyl phenol) blends: 1. Predictions based on low molecular weight analogs. *Polymer* 1992; 33(4):755-759.
- [35] Machado JM and French RN. Miscible polyacetal-poly(vinyl phenol) blends: 2. Thermomechanical properties and morphology. *Polymer* 1992; 33 (4): 760-766 .

[36] Adam G, Gibbs JH. On the Temperature Dependence of Cooperative Relaxation Properties in Glass-Forming Liquids. *J Chem Phys* 1965; 43: 139-146.

[37] Kerasidou A, Psarras GC, Siengchin S, Karahaliou PK, Xanthopoulos N, Georga SN, Krontiras CA and Karger-Kocsis J. Polyoxymethylene (POM) based nanocomposites: Morphology, dielectric response and energy storage efficiency. In: Proceedings of the 28th Pan-Hellenic Conference on Solid State Physics and Materials Science. Patras, Greece; 2012.

[38] Psarras GC, Gatos KG, Karahaliou PK, Georga SN, Krontiras CA, Karger-Kocsis J. Relaxation phenomena in rubber/layered silicate nanocomposites. *Express Polym Lett* 2007; 1(12): 837–845.

[39] Kakizaki M and Hideshima T. Multiple relaxation in  $\alpha$ - and  $\gamma$ - loss bands in polyethylene. *J Macromol Sci-Phys* 1973; B8(3-4):367-387.

[40] Hedvig P. Basic principles of dielectric spectroscopy. In: Dielectric spectroscopy of polymers. Budapest: Adam Hilger Ltd Bristol, Akadémiai Kiadó; 1977. p. 27-30.

[41] Danch A, Osoba W, Chrobak D, Nowaczyk G and Jurga S.  $\alpha_c$  relaxation of the constrained amorphous phase Polyethylene-chalk composites. *J Therm Anal Cal* 2007; 90; 201–208.

[42] Frübing P, Blischke D, Gerhard-Multhaupt R and Salah Khalil M. Complete relaxation map of polyethylene: filler-induced chemical modifications as dielectric probes. *J Phys D: Appl Phys* 2001; 34:3051–3057.

[43] Peponi L, Puglia D, Torre L, Valentini L, Kenny JM. Processing of nanostructured polymers and advanced polymeric based nanocomposites. *Mater Sci Eng R* 2014; 85: 1-46.

[44] Esposito Corcione C, Manera MG, Maffezzoli A, Rella R. Synthesis and characterization of optically transparent epoxy matrix nanocomposites. *Mater Sci Eng C* 2009; 29: 1798-1802.

[45] Halbach T S, Mülhaupt R. Boehmite-based polyethylene nanocomposites prepared by in-situ polymerization. *Polymer*; 49: 867-876.

## Figure Captions

**Fig. 1.** Frequency – temperature variation of the loss tangent ( $\tan\delta$ ) for (a) pure POM, (b) POM/alumina and (c) POM/LS systems.

**Fig. 2.** Comparative isothermal plots of the imaginary part of the electric modulus ( $M''$ ) as a function of frequency, at three different temperatures in the low temperature region for all three studied systems at: (a)  $-70\text{ }^{\circ}\text{C}$ , (b)  $-50\text{ }^{\circ}\text{C}$  and (c)  $-20\text{ }^{\circ}\text{C}$ .

**Fig. 3.** Comparative isothermal plots of the imaginary part of the electric modulus ( $M''$ ) as a function of frequency, at three different temperatures in the high temperature region for all three studied systems at: (a)  $100\text{ }^{\circ}\text{C}$ , (b)  $120\text{ }^{\circ}\text{C}$  and (c)  $150\text{ }^{\circ}\text{C}$ .

**Fig. 4.** Comparative isochronal plots of the imaginary part of the electric modulus ( $M''$ ) as a function of temperature, at two different frequencies for all three studied systems at: (a)  $0.1\text{ Hz}$  and (b)  $1\text{ kHz}$ .

**Fig. 5.** Loss peak frequency maxima as a function of inverse temperature, for all the examined specimens and for  $\alpha$ -,  $\beta$ -  $\gamma$ - and  $\delta$ - relaxation processes, as detected in the  $M''$  versus frequency spectra. Solid lines are produced by fitting Eqns (1) and (2) to the experimental data.

**Fig. 6.** (a) Frequency-temperature variation of the imaginary part of the electric modulus ( $M''$ ) for all three studied systems, (b) Combined Cole-Cole plots for selected temperatures of each sample (—POM, —POM/alumina, —POM/LS).



Figures

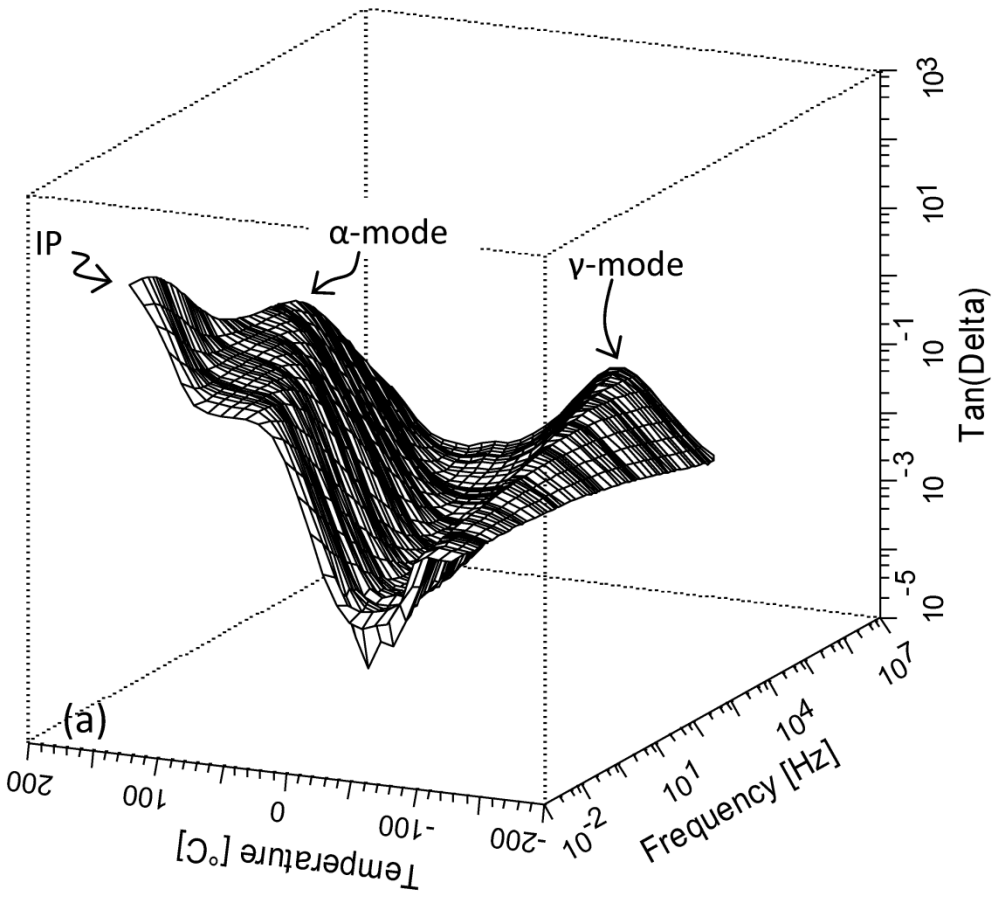


Fig.1a

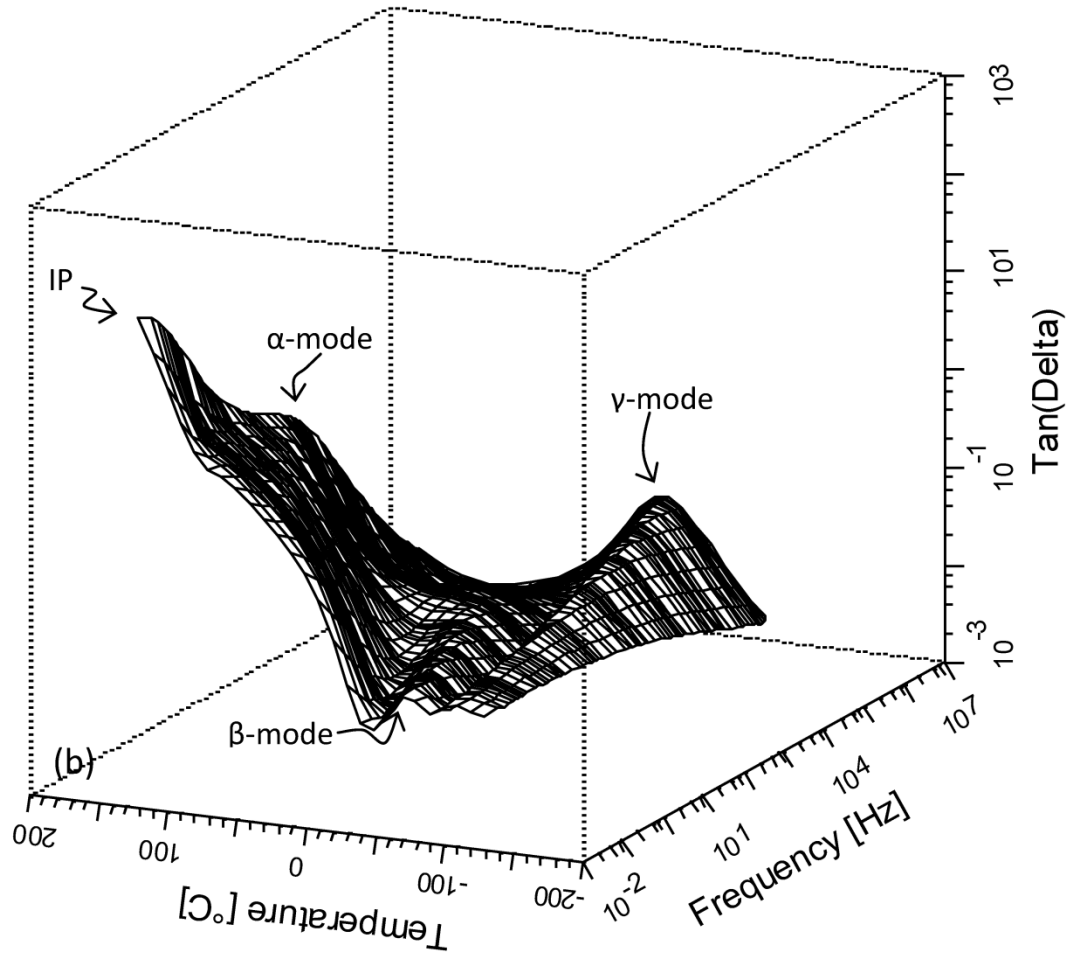


Fig.1b

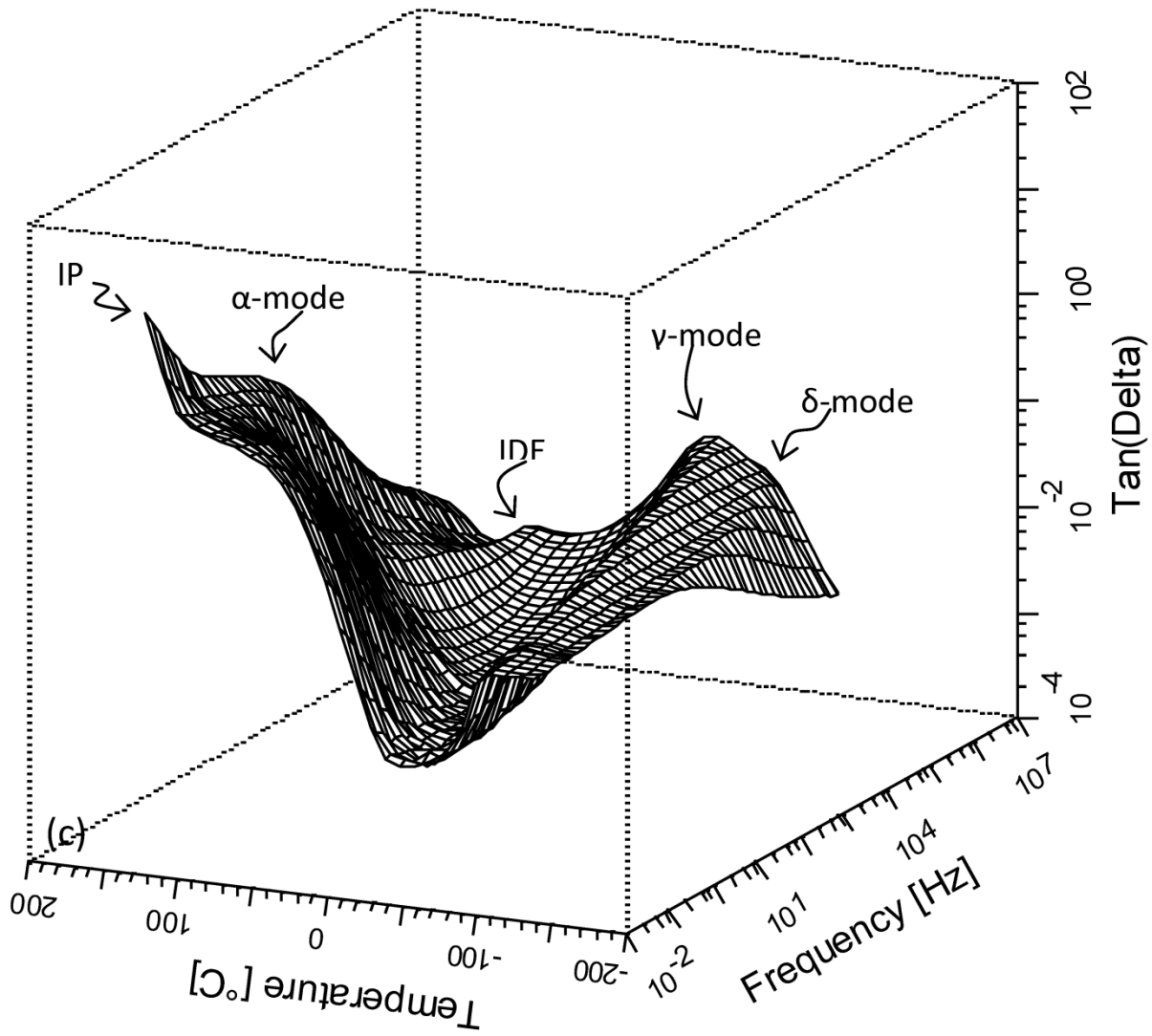


Fig.1c

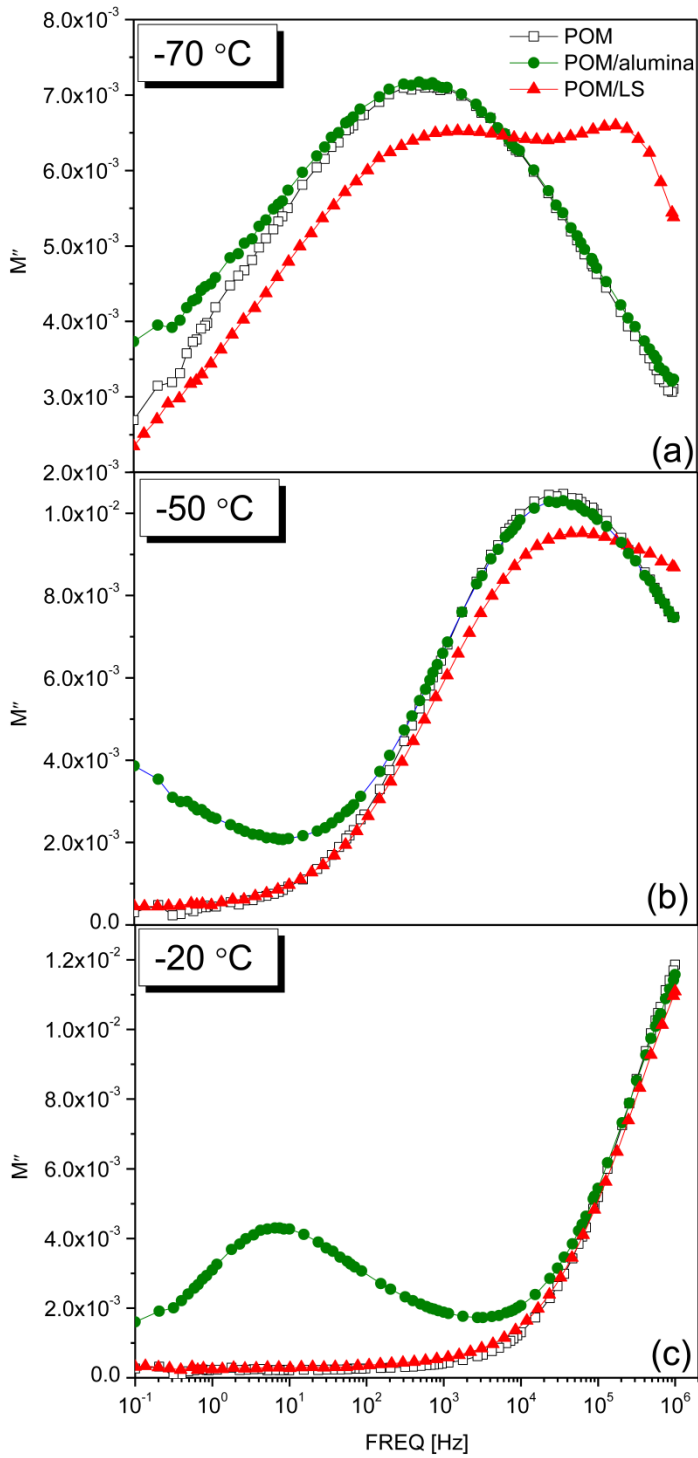


Fig.2

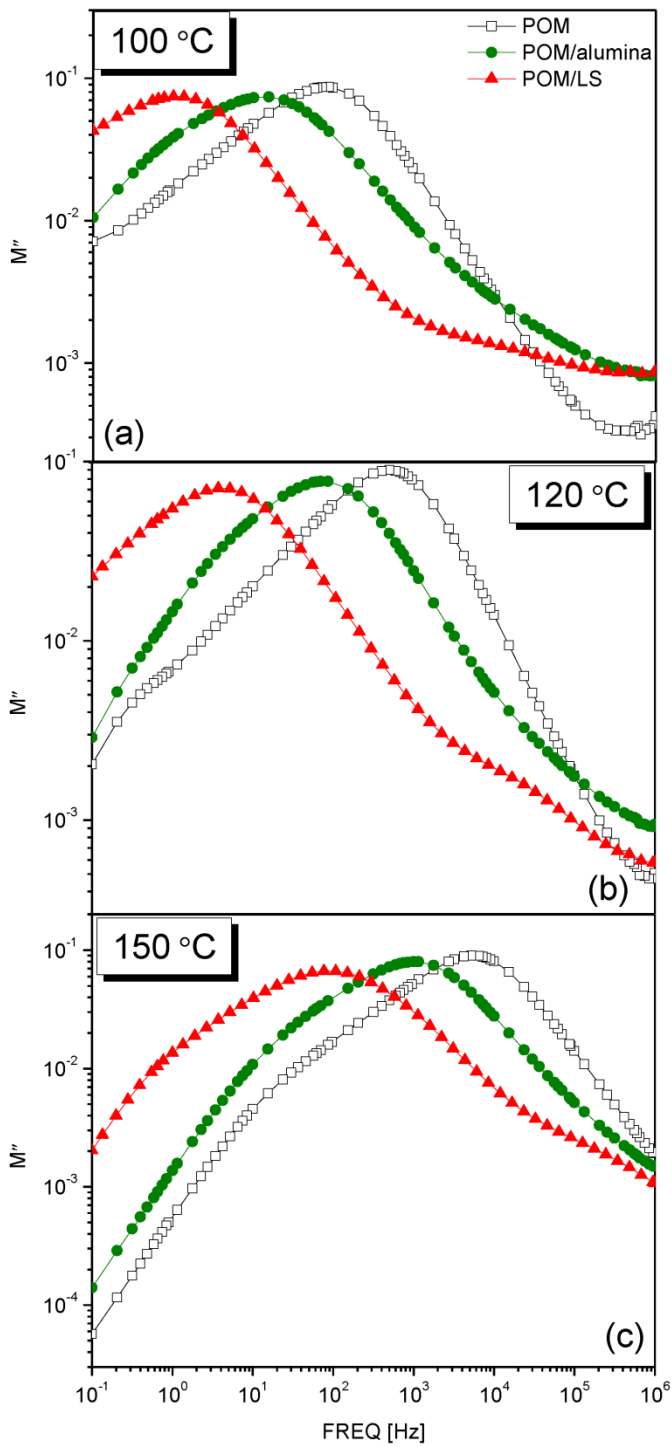


Fig.3

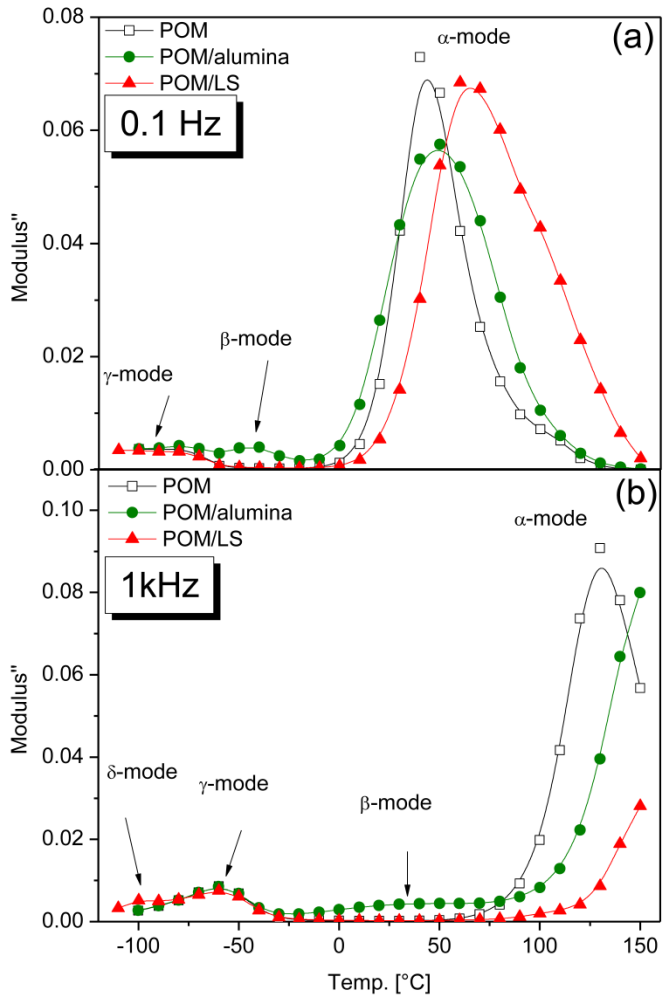


Fig.4

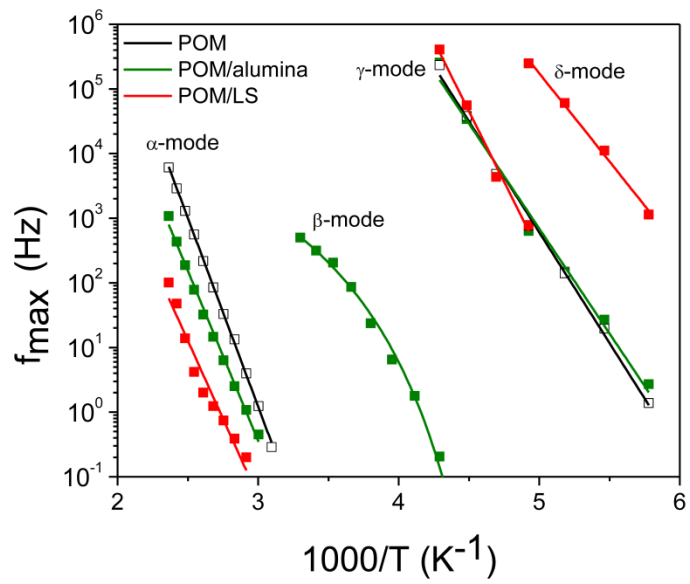


Fig.5

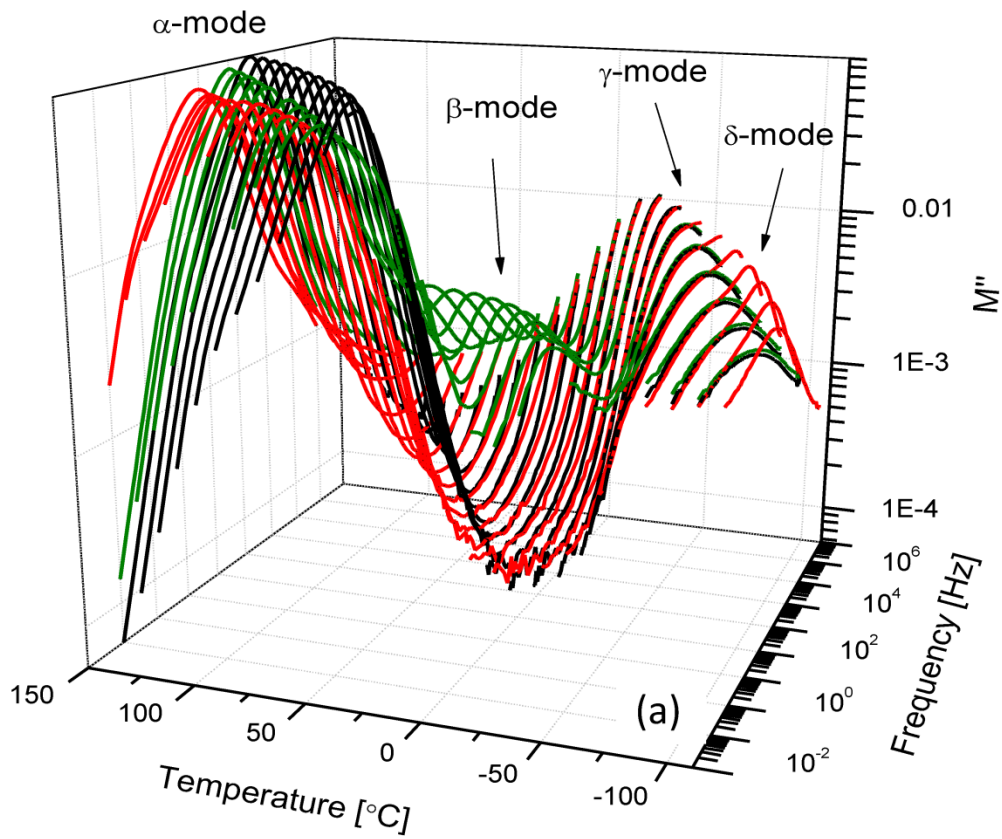


Fig.6a

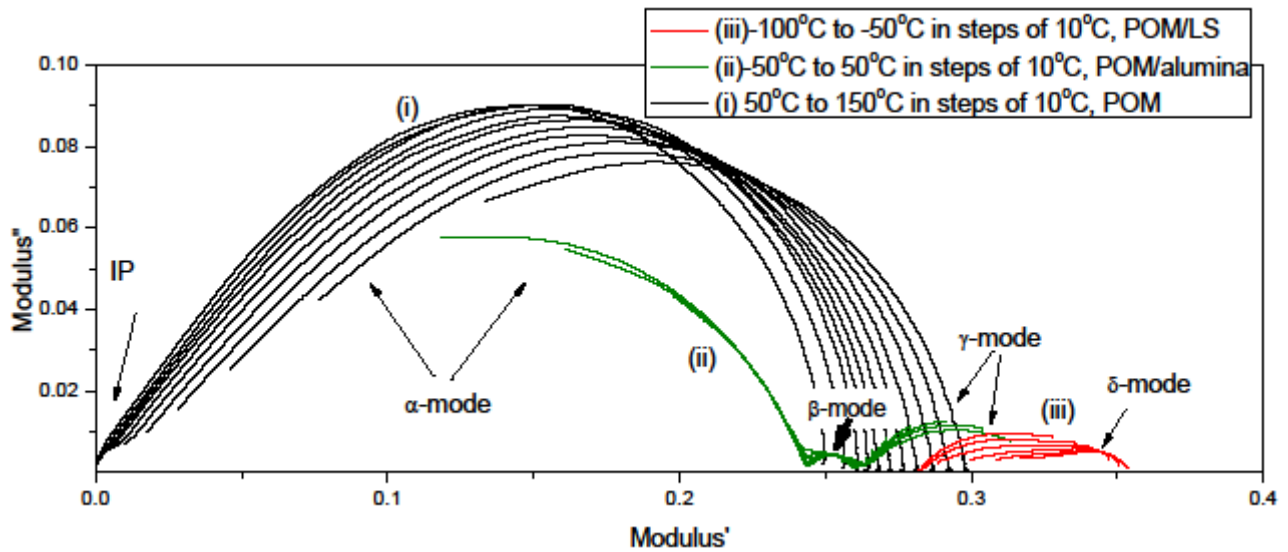


Fig.6b